

pubs.acs.org/acscatalysis Research Article

Impact of Alkyl Core Substitution Kinetics in Diaryl Dihydrophenazine Photoredox Catalysts on Properties and Performance in O-ATRP

Katherine O. Puffer, Daniel A. Corbin, and Garret M. Miyake*



Cite This: ACS Catal. 2023, 13, 14042-14051



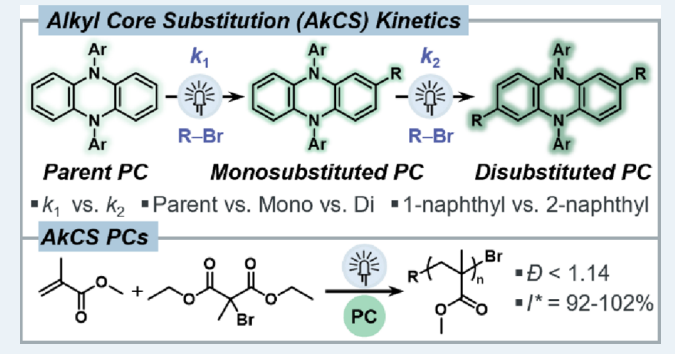
ACCESS I

III Metrics & More

Article Recommendations

s Supporting Information

ABSTRACT: Organocatalyzed atom transfer radical polymerization (O-ATRP) is a controlled radical polymerization method mediated by organic photoredox catalysts (PCs) for producing polymers with well-defined structures. While N_iN -diaryl dihydrophenazine PCs have successfully produced polymers with low dispersity (D < 1.3) in O-ATRP, low initiator efficiencies ($I^* \sim 60-80\%$) indicate an inability to achieve targeted molecular weights and have been attributed to the addition of radicals to the PC core. In this work, we measure the rates of alkyl core substitution (AkCS) to gain insight into why PCs differing in N-aryl group connectivity exhibit differences in polymerization control. Additionally, we evaluate how PC properties evolve during O-ATRP when a non-core-substituted PC is used. PC 1



with 1-naphthyl groups in the *N*-aryl position resulted in faster AkCS ($k_1 = 1.21 \pm 0.16 \times 10^{-3} \, \text{s}^{-1}$, $k_2 = 2.04 \pm 0.11 \times 10^{-3} \, \text{s}^{-1}$) and better polymerization control at early reaction times as indicated by plots of molecular weight (number average molecular weight = $M_{\rm n}$) vs conversion compared to PC 2 with 2-naphthyl groups ($k_1 = 6.28 \pm 0.38 \times 10^{-4} \, \text{s}^{-1}$, $k_2 = 1.15 \pm 0.07 \times 10^{-3} \, \text{s}^{-1}$). The differences in rates indicate that *N*-aryl connectivity can influence polymerization control by changing the rate of AkCS PC formation. The rate of AkCS increased from the initial to the second substitution, suggesting that PC properties are modified by AkCS. Increased PC radical cation (PC*) oxidation potentials ($E_{1/2} = 0.26 - 0.27 \, \text{V}$ vs SCE) or longer triplet excited-state lifetimes ($\tau_{T1} = 1.4 - 33 \, \mu \text{s}$) for AkCS PCs 1b and 2b compared to parent PCs 1 and 2 ($E_{1/2} = 0.21 - 0.22 \, \text{V}$ vs SCE, $\tau_{T1} = 0.61 - 3.3 \, \mu \text{s}$) were observed and may explain changes to PC performance with AkCS. Insight from evaluation of the formation, properties, and performance of AkCS PCs will facilitate their use in O-ATRP and in other PC-driven organic transformations.

KEYWORDS: catalysts, photocatalysts, polymerization, polymers, radical polymerization

■ INTRODUCTION

Photoredox catalysis is an approach to chemical transformations that employs a catalyst activated by light to initiate redox chemistry and access unique chemical transformations under mild reaction conditions. 1-4 PC-mediated syntheses can be more energy-efficient relative to typical thermally driven methods, allow for spatial and temporal control, access unique reaction pathways, and can provide selective reactivity. In photoredox catalysis, photoexcitation results in an excited-state PC (PC*) that is more reducing or oxidizing relative to the ground-state PC and can engage in single-electron transfer (SET) or energy transfer, provided that it is sufficiently longlived for a bimolecular reaction to occur.⁶⁻⁸ Therefore, both the photophysical and redox properties of the PC are essential to performance. Substantial progress in photoredox catalysis has largely used Ru and Ir complexes, which are notable for strong visible-light absorption, near-unity triplet quantum yield $(\Phi_{\rm ISC})$, and redox stability.^{2,6} Despite their utility, Ru and Ir PCs are dependent on rare-earth metals. 10 If organic PCs can

provide competitive photophysical and redox properties, they have the potential to serve as sustainable alternatives to precious-metal-based PCs. 11–15 Use of metal-based catalysts in polymerizations can present additional challenges including incompatibility with certain reagents and contamination of the final polymer product. For example, atom transfer radical polymerization (ATRP) is a popular controlled radical polymerization (CRP) method that employs transition metal catalysts such as Cu¹⁶ or Ru¹⁷ to produce well-defined polymers. However, metal contamination of the polymer matrix can limit ATRP's use in certain metal-sensitive

Received: August 28, 2023 Revised: September 26, 2023 Published: October 18, 2023





electronic or biomedical applications. ^{18–20} Additionally, traditional ATRP may not be suitable for monomers that strongly interact with metal catalysts. ^{18,21}

O-ATRP is a variant of ATRP that employs organic PCs and light to mediate a controlled polymerization. Consequently, O-ATRP eliminates metal contamination and can provide access to monomers that coordinate to metal catalysts while allowing for spatial and temporal control. ^{12,19} As a CRP technique, O-ATRP allows for the synthesis of polymers with precisely tailored molecular weights, compositions, and architectures. Well-defined polymer structures are necessary for applications including drug delivery, surface functionalization, and more. ^{22–24} To achieve polymerization control, O-ATRP mediates an equilibrium between the activation and deactivation of a growing polymer chain (Figure 1). Activation

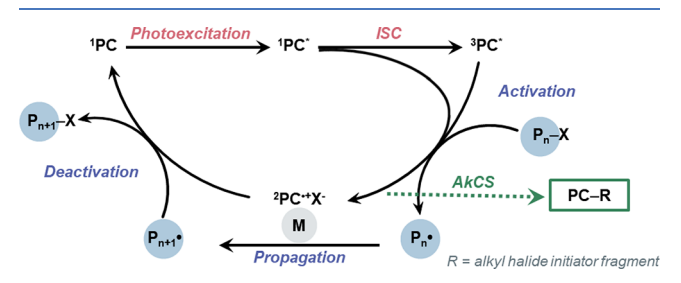


Figure 1. Proposed mechanism for O-ATRP, proceeding through an oxidative quenching photoredox pathway.

by PC* is followed by rapid deactivation by the PC*, resulting in a low concentration of radicals and minimizing undesirable bimolecular radical termination reactions, which contribute to a high D (>1.5) and nonunity I^* . Adequate PC* reduction potentials $[E^{\circ}(^2PC^{\bullet+}/^nPC^*)]$ and $PC^{\bullet+}$ oxidation potentials $[E^{\circ}(^2PC^{\bullet+}/^nPC^*)]$ are therefore critical aspects of PC design. ^{25,26} For activation, the excited-state reduction potential $[E^{\circ}(^2PC^{\bullet+}/^nPC^*)]$ of the PC must be sufficiently negative to reduce the C–Br bond of either an alkyl halide initiator or a

deactivated polymer chain end $([E^{\circ}(^{2}PC^{\bullet+}/^{n}PC^{*})] < -0.6$ to -0.8 V vs SCE). For deactivation, the PC $^{\bullet+}$ must have an oxidation potential positive enough to rapidly oxidize the propagating polymer radical, forming a halide-capped polymer $(E^{\circ}(^{2}PC^{\bullet+}/^{1}PC) > -0.8 \text{ V vs SCE})$ and regenerating the ground-state PC. Photophysical properties including molar absorptivity ($\varepsilon_{\mathrm{max,abs}}$), wavelength of maximum absorption $(\lambda_{\text{max abs}})$, charge transfer (CT) character, and excited-state lifetimes (τ) have also been found to be catalytically relevant and influence polymerization control. 6,19,27 Since the seminal reports of O-ATRP in 2014 with the use of perylene²⁸ and 10phenyl phenothiazine²¹ as PCs for O-ATRP, several new families of highly reducing organic PCs have been used, including phenoxazines, 13 dihydrophenazines, 12 dihydroacridines,²⁹ and other phenochalcogenazines.³⁰ This work focuses on dihydrophenazine PCs, which are notable for their highly reducing excited state and good polymerization control (D <

O-ATRP with dihydrophenazine PCs has proven to be a robust method for producing polymers with low D, but in early work, I* was typically 60-80%, which indicates an inability to achieve targeted molecular weights. 12 It was hypothesized that the observed low I^* is a result of initiator-derived alkyl radicals adding to the PC core, which prevents initiation and growth of the predicted number of polymer chains.³¹ More recent work identified aryl core substitution (ArCS) as an approach to modify PC properties and improve I^* by blocking the positions available for addition of alkyl radicals to the PC core. 32,33 In these studies, ArCS PCs were observed to have near-unity I* and facilitate control with low PC loadings in O-ATRP (5-50 ppm). Notably, low PC loadings simplify polymer purification and lower reagent costs, improving the overall utility of O-ATRP. 32,33 In another work, core substitution by radical addition of alkyl halide initiator fragments was investigated through the reaction of N,N-di(2-naphthyl)-5,10-dihydrophenazine (PC 2) and diethyl 2-bromo-2-methylmalonate (DBMM) (Figure 2).31 Through model reactions and

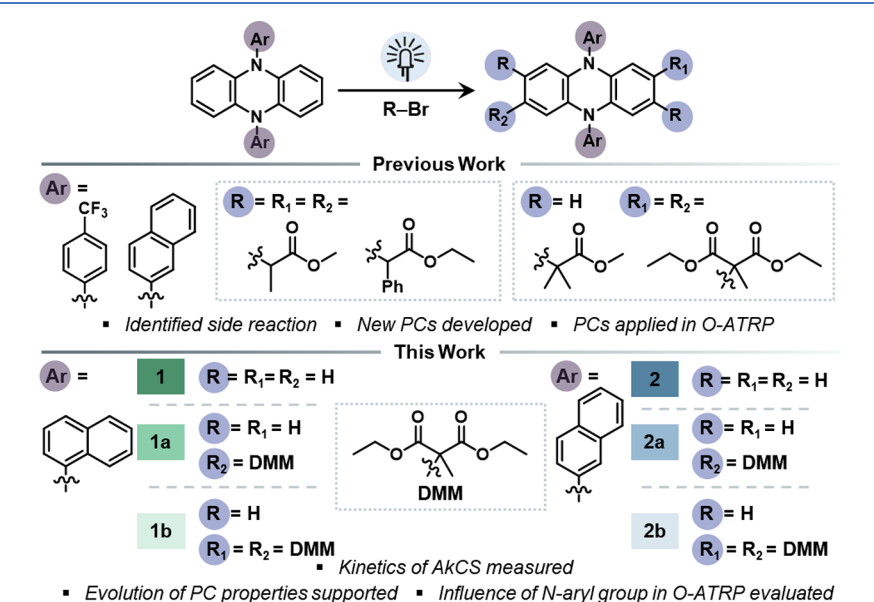


Figure 2. General schematic of the AkCS reaction (top), previous work on AkCS (middle), and PCs explored in this work (bottom). DMM = alkyl fragment of diethyl 2-bromo-2-methylmalonate, diethyl 2-methylmalonate. Note that while the PC 2, 3, 7, and 8 positions can all undergo monosubstitution and disubstitution produces a mixture of 2- and 7- and 3- and 7-regioisomers, one isomer is depicted here for simplicity in both cases. See the SI for reaction conditions.

spectroscopic studies, it was found that alkyl radicals generated from the initiator add twice to the core of PC 2 and that O-ATRP mediated by an AkCS PC results in $I^* \sim 100\%$. Additionally, the AkCS side reaction was leveraged to create core-substituted PCs that mediated the polymerization of acrylate monomers via O-ATRP with moderate to good control (D = 1.15 - 1.45, $I^* = 83 - 127\%$). In a following paper, AkCS was explored further through investigation of the reaction between 5,10-di(4-trifluoromethylphenyl)-5,10-dihydrophenazine and four alkyl bromide O-ATRP initiators (Figure 2).³⁴ AkCS was found to alter PC photophysical and redox properties, and model reactions were used to improve the mechanistic understanding of addition to the PC core by alkyl halide-derived radicals. In the proposed mechanism, the PC* reduces an alkyl halide initiator to produce an alkyl radical and Br-. The alkyl radical then adds to the PC core, which is subsequently deprotonated to form a monosubstituted PC. If more initiator is available, the monosubstituted PC will then repeat the AkCS process for further substitutions.³⁴ Furthermore, AkCS combined with decreased solvent polarity was found to enable low PC loadings with moderate control (D =1.36, $I^* = 107\%$) at 10 ppm. Similarly, Zhang et al. explored AkCS with 5,10-di(4-methoxyphenyl)-5,10-dihydrophenazine and several alkyl halide initiators and observed improved I* for most AkCS PCs.35

The changes to PC properties and polymerization outcomes observed with AkCS highlight the importance of evaluating the kinetics of AkCS. In the work described herein, we measured the rate at which the core-substituted PC is formed and begins to mediate the polymerization in place of the parent PC (Figure 2). The rate of substitution was found to increase from the first to second substitution, indicating an evolution of PC properties that was supported through PC characterization. Additionally, PCs with *N*-aryl groups differing only in naphthyl connectivity had inequivalent rates of substitution, providing insight into why they perform differently in O-ATRP. Overall, this work provides a fundamental understanding into how AkCS influences polymerization outcomes through the examination of the substitution rate and PC property evolution.

RESULTS AND DISCUSSION

AkCS Kinetic Studies. While prior work demonstrated the impact of AkCS on PC properties and performance in O-ATRP and explored the mechanism of radical addition of alkyl halide initiator fragments to the core of N,N-diaryl dihydrophenazine PCs, 31,34 the studies herein demonstrate the importance of the rate at which AkCS is occurring on reaction outcomes. A previous study on AkCS showed that PC properties including molar absorptivity ($arepsilon_{ ext{max,abs}}$), wavelength of maximum absorption ($\lambda_{\text{max,abs}}$), wavelength of maximum emission ($\lambda_{\text{max,em}}$), and redox potentials are altered by AkCS, as are polymerization outcomes (increased I^*).³⁴ Both observations suggest that the PC properties are evolving over the course of the polymerization when parent PCs are used. We proposed that a further understanding of the rate of AkCS and the properties of AkCS PCs would provide insight into why certain PCs impart superior polymerization control in the O-ATRP despite similar structures. Specifically, we hypothesized that the PC N-aryl group identity will impact the rate of substitution and that differences in substitution rates can explain differences in PC performance. PCs 1 and 2, differing only in the connectivity of their N-aryl groups, have been

reported to perform inequivalently in O-ATRP. 12,36 It is unclear from prior work which photophysical and redox properties account for the observed differences. The rates of AkCS for PCs 1 and 2 are inequivalent, then PC properties will evolve more quickly for one PC, potentially explaining differences in polymerization outcomes. Alternatively, the final properties of the AkCS PC may determine polymerization control regardless of the speed with which they are accessed.

To explore the hypothesis presented above, we targeted the substitution of PCs 1 and 2 by the alkyl halide initiator DBMM. DBMM fragments (R*) were found to substitute the core of dihydrophenazine PCs twice to produce a disubstituted PC in prior work (combination of 2- and 7- and 3- and 7regioisomers).³⁴ Tetra- versus disubstitution was determined by the sterics of the initiator, with bulkier tertiary alkyl bromide initiators including DBMM resulting in disubstitution. We hypothesized that for PCs 1 and 2, as sequential substitutions to the PC core by R° occur, each substitution product and rate constant could be isolated. In preparation for the kinetic experiments, PCs 1, 1a, 1b, 2, 2a, and 2b were synthesized. Each derivative of the parent PC (monosubstituted PCs 1a and 2a and disubstituted PCs 1b and 2b) was isolated and found to have distinct ¹H NMR spectra (Figures S8, S10, S12, and S14). The distinct spectra observed for the monosubstituted and disubstituted PCs indicated that the rate constants for substitution could be determined by following the reaction between R^o and PCs 1 or 2 via ¹H NMR.

The rate constants for the first substitution (k_1) were measured by irradiating PC 1 or 2 with DBMM in *N,N*-dimethylacetamide (DMAc) and monitoring the conversion to PCs 1a and 2a over time. The first substitution followed linear pseudo-first-order kinetics, from which the rate constant k_1 was determined (Figure 3). By lowering the concentration of the initiator relative to PC from excess to stoichiometric ([PC] = [DBMM] = 1.53 mM), the first substitution was promoted over the second. For determination of the rate constants for

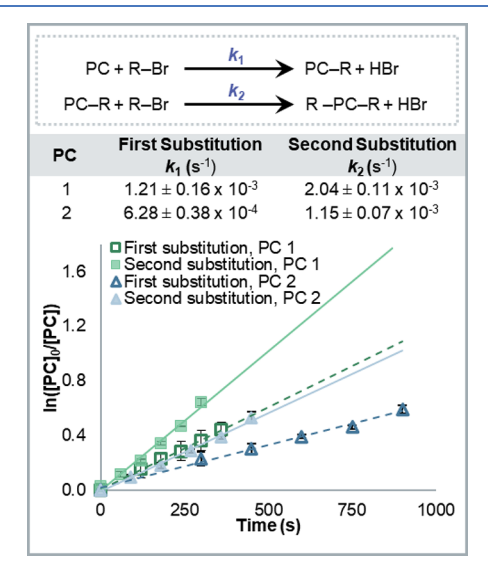


Figure 3. Pseudo-first-order kinetic plots from time points analyzed by 1H NMR for the first and second substitution of PC **1** and PC **2** by R $^{\bullet}$. Conditions: [DBMM]:[PC] = [1]:[1] in 7.50 mL of DMAc. AkCS was run with a white LED beaker as the light source (see the SI for more information). Rate constants for each substitution reaction were obtained from the slope of PC consumption ($\ln[PC]_0/[PC]$) vs time.

Table 1. Summary of the Photophysical Properties for PCs

PC	$\lambda_{\text{max,abs}} (\text{nm})^a$	$\varepsilon_{\text{max,ab}} \ (\text{M}^{-1}\text{cm}^{-1})^a$	$\lambda_{\text{max,em}} (\text{nm})^b$	Stokes shift $(nm)^c$	$E_{\rm S1,exp}~({\rm eV})^d$	$E_{\rm T1,exp} \ ({\rm eV})^d$	$\tau_{S1} (ns)^e$	$ au_{\mathrm{T1}} \ (\mu \mathrm{s})^e$	$\Phi_{\mathrm{f}} \left(\%\right)^{f}$
1	362	4300	645	283	1.92	2.24	8.5	0.61	1.30
1b	365	6800	629	264	1.97	2.23	10	1.4	2.10
2	343	7100	640	297	1.93	2.34	4.0 ^g	3.3	0.56
2b	350	8500	623	273	1.99	2.30	7.9	33	1.74

"Measured by UV-vis spectroscopy in DMAc. "Measured by steady-state fluorescence spectroscopy in DMAc. "Stokes shift = $\lambda_{\text{max,em}} - \lambda_{\text{max,abs'}}$ and E_{S1} and E_{T1} (eV) = 1239.8/ λ (nm); calculated from $\lambda_{\text{max,em}}$ from fluorescence (measured at room temperature) and phosphorescence (measured at 77 K), respectively. "Determined by transient absorption spectroscopy." Measured in DMAC by absolute methods. "Measured by time-correlated single-photon counting in DMAc.

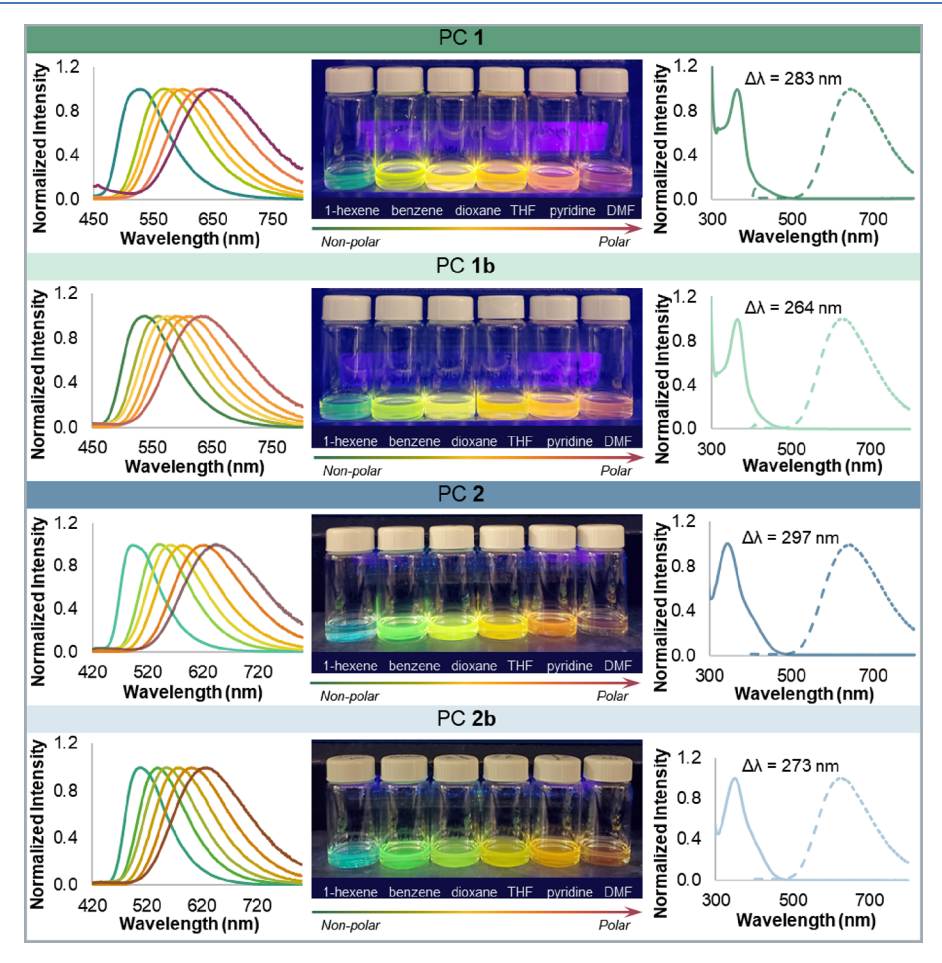


Figure 4. From left to right, overlaid emission profiles of PCs in different polarity solvents, photographs of the PCs dissolved in solvents of increasing polarities under UV-light irradiation, and overlaid normalized absorption (solid line) and emission (dotted line) spectra acquired in DMAc

the second substitution (k_2) , the same reaction conditions for the first substitution were applied starting from monosubstituted PC 1a or 2a ([PC] = [DBMM] = 1.53 mM). The second substitution followed linear pseudo-first-order kinetics from which the rate constant k_2 was determined (Figure 3). Notably, time points taken after ~50% conversion deviated from linear pseudo-first-order kinetics for both substitutions, suggesting that as the DBMM concentration lowers, pseudo-first-order kinetics may no longer be a good approximation. For the AkCS reaction, activation was predicted to be rate-limiting, and the concentration of DBMM was assumed to be very high relative to the concentration of PC*. However, as DBMM is consumed, it may no longer be in large enough excess compared to PC* for this pseudo-first-order assumption to be accurate. To address this possibility, all time points were

taken before 50% conversion. A pseudo-first-order kinetic model was developed using the assumption that activation is the rate-limiting step (Figure S29). The concentration of PC over time predicted by the model closely matched the experimentally measured concentrations, supporting this initial hypothesis of activation as the rate-limiting step (Figure S30). Alternatively, radical addition of R[•] to PC^{•+} could be the rate-limiting step instead of SET, in which case second-order kinetics would apply (Figures S31 and S32). To support that AkCS of the PCs is a light-driven reaction, control reactions were performed under standard reaction conditions in the dark, and negligible AkCS was observed (Figures S25–S28).

Contrary to our initial prediction that the first substitution would be faster than the second due to the increased number of positions available for substitution, for PC 1, k_1 = 1.21 \pm

 $0.16 \times 10^{-3} \text{s}^{-1}$ and $k_2 = 2.04 \pm 0.11 \times 10^{-3} \text{ s}^{-1}$. This same trend was observed for PC 2 ($k_1 = 6.28 \pm 0.38 \times 10^{-4} \text{ s}^{-1}$, $k_2 =$ $1.15 \pm 0.07 \times 10^{-3} \text{ s}^{-1}$). The increase in the AkCS rate after the first substitution suggests that an evolution of PC properties occurs on this timescale during O-ATRP. In particular, the observed rate increases may indicate modification to properties that influence the excited-state reduction potential $(\bar{E}^{\circ*})$ or $PC^{\bullet+}$ oxidation potential $(E_{1/2})$. Access to PC properties that facilitate either SET or radical addition, depending on which step is rate-limiting, would result in a faster second substitution of PC by R* due to the increased thermodynamic driving force for AkCS. Additionally, these results show that changes to PC properties are happening at early reaction times relative to O-ATRP, which typically reaches high conversions between 8 and 24 h depending on solvent polarity.^{31,36} The AkCS reactions reach ~50% conversion between 5 and 15 min, much shorter than the timescale of O-ATRP. The timescale of AkCS suggests that AkCS PCs mediate most of the polymerization. Importantly, AkCS PCs have different properties from non-AkCS PCs, so AkCS PC properties are overall more important for governing polymerization control.

Comparing PC 1 and PC 2, PC 1 undergoes AkCS faster than PC 2 $(k_1 = 1.21 \pm 0.16 \times 10^{-3} \text{ s}^{-1} \text{ for } 1, k_1 = 6.28 \pm 0.38$ $\times 10^{-4} \text{ s}^{-1}$ for 2). Similarly, PC 1a $(k_2 = 2.04 \pm 0.11 \times 10^{-3})$ s⁻¹) is substituted faster than 2a $(k_2 = 1.15 \pm 0.07 \times 10^{-3} \text{ s}^{-1})$. We initially hypothesized that the increased sterics of PC 1 would inhibit core substitution and slow the rate of AkCS compared to PC 2, but instead, PC properties may determine the rate of core substitution. In previous work, it has been observed that PC 1 mediates O-ATRP with a faster polymerization rate than PC 2, consistent with the trend observed here for AkCS.¹² Overall, the results from the kinetic experiments support the hypothesis that the N-aryl group will influence the rate of substitution, but further investigation is needed to determine why the 1-naphthyl group in PC 1 significantly increases the rate over 2-naphthyl in PC 2. However, the increased rate of AkCS for PC 1 and faster access to improved PC properties could explain why it has historically exhibited better polymerization control in O-ATRP than PC 2 (see below).36,38

Photophysical and Redox Characterization of PCs. The observed increase in the rate between the first and second substitution led us to hypothesize that AkCS is modifying PC properties at the beginning of O-ATRP with PCs 1 and 2. To quantify the change in PC properties with AkCS, the photophysical and redox properties of the PCs were measured. In previous studies with dihydrophenazine PCs, AkCS has been found to impact and often improve catalytically relevant properties including $\varepsilon_{\text{max,abs}}$, PC* $E_{1/2}$, and $E^{\circ*}$, which impact polymerization control in O-ATRP. We predicted that similar improvements to PC properties would be observed with AkCS of PCs 1 and 2.

Steady-State Absorption and Emission Spectroscopy. PC $\varepsilon_{\text{max,abs}}$ and $\lambda_{\text{max,abs}}$ both are reported to influence PC performance in O-ATRP. Compared to PCs 1 and 2 ($\varepsilon_{\text{max,abs}} = 4300 \text{ M}^{-1}\text{cm}^{-1}$ for 1, 7100 M $^{-1}\text{cm}^{-1}$ for 2), AkCS PCs 1b and 2b exhibit higher molar absorptivities ($\varepsilon_{\text{max,abs}} = 6800 \text{ M}^{-1}\text{cm}^{-1}$ for 1b, 8500 M $^{-1}\text{cm}^{-1}$ for 2b) and have slightly redshifted $\lambda_{\text{max,abs}}$ (Table 1). The high $\varepsilon_{\text{max,abs}}$ observed for PC 2b is notable because a higher $\varepsilon_{\text{max,abs}}$ indicates an increase in the efficiency of photoexcitation and is typically correlated to better PC performance in the O-ATRP due to an increased

excited-state population. Examining the influence of AkCS on emission, it was found that $\lambda_{\text{max,em}}$ is blueshifted from parent PCs 1 and 2 ($\lambda_{\text{max,em}} = 645 \text{ nm for 1}$, $\lambda_{\text{max,em}} = 640 \text{ nm for 2}$) to AkCS PCs 1b and 2b ($\lambda_{\text{max,em}} = 629 \text{ nm}$ for 1b, $\lambda_{\text{max,em}} = 623$ nm for 2b) (Figure 4). The observed changes in $\lambda_{\text{max,abs}}$ and $\lambda_{\text{max.em}}$ indicate that AkCS of PCs 1 and 2 by R $^{\bullet}$ stabilizes the π^* orbitals involved in light absorption (S_n) or the ground state (S_0) while destabilizing the lowest energy (S_1) π^* orbitals involved in emission, which are likely CT states (see below for discussion of CT states). Consideration of the higher singlet excited-state energies $(E_{\rm S1,exp})$ observed for AkCS PCs provides additional evidence of a slightly higher energy CT state. AkCS PC 1b had a 0.05 eV increase in E_{S1} from PC 1, while AkCS PC **2b** had a 0.06 eV increase in E_{S1} from PC **2**. Overall, the change in absorption and emission of the PCs after AkCS supports the hypothesis that PC properties are modified with AkCS and therefore likely evolve during O-ATRP.

As a result of their blueshifted $\lambda_{\text{max,em}}$ and redshifted $\lambda_{\text{max,abs}}$, AkCS PCs display a smaller Stokes shift $(\Delta \lambda = \lambda_{\text{max.em}})$ $\lambda_{\text{max.abs}}$) than that of the corresponding parent PCs ($\Delta \lambda = 264$ nm for **1b** and 273 nm for **2b**, $\Delta \lambda = 283$ nm for **1** and 297 nm for 2). The Stokes shift provides insight into the CT character of the PC, with a large Stokes shift typically indicating CT character. PCs that access CT excited states have been found to perform better in O-ATRP than locally excited (LE) PCs, which we posit is due to CT facilitating ISC to longer-lived triplet excited states³⁹ and enhanced electron transfer rates by consolidation of electron density.³⁸ While all the PCs herein exhibit broad and featureless emission profiles indicative of CT, the slight reduction of the Stokes shift in AkCS PCs compared to the parent PCs suggests that AkCS is altering either the energy or character of the CT singlet state (Figure 4). To further evaluate the CT character of the PCs through solvatochromism, emission spectra were obtained in solvents of varied polarity. Consistent with the measured Stokes shifts, while the AkCS PCs displayed solvatochromism, the extent of solvatochromism was smaller than that in the corresponding parent PC (Figure 4). Since solvatochromism in dihydrophenazine PCs arises from the stabilization of polar CT states by polar solvents and causes redshifted emission, 36,38 this piece of data reinforces that AkCS PCs retain CT states, but the energetics of the CT state is altered by the core substituents.

Next, we measured the PC triplet energies $(E_{T1,exp},$ determined from the $\lambda_{\text{max,em}}$ of phosphorescence measured at 77 K), which were all found to be higher than the E_{S1} measured at room temperature for each PC. While typically, $E_{\rm S1}$ is higher or close to isoenergetic with the $E_{\rm T1}$ in dihydrophenazine PCs, ⁴⁰ the observed increase from $E_{\rm S1}$ to $E_{\rm T1}$ is likely because $E_{\rm T1}$ was measured at 77 K, limiting internal conversion to a lower energy singlet state before ISC and within the triplet state after ISC. In the AkCS PCs, E_{T1} was higher for the PC 2 compared to PC 1 (E_{T1} = 2.24 eV for 1, $E_{\rm T1}$ = 2.34 eV for 2) and higher for PC 2b compared to PC 1b $(E_{\text{T1}} = 2.23 \text{ eV for } 1b, E_{\text{T1}} = 2.30 \text{ eV for } 2b)$. Conclusions about the lowest energy triplet state (T1) cannot be made based on these results, but they suggest that the initial states occupied after ISC (T_n) in the PC 2 family are higher than those in the PC 1 family. Additionally, while AkCS raises E_{S1} , it appears to lower E_{T1} of the state accessed after ISC.

To evaluate decay pathways from the singlet excited state that compete with ISC or SET, the quantum yield of fluorescence (Φ_f) was measured. For all the PCs characterized, the Φ_f was low (0.56–2.10%), suggesting that radiative decay

through fluorescence is not a primary decay pathway. However, the AkCS PCs were found to have higher Φ_f than their respective parent PCs (ex. $\Phi_f=1.30\%$ for 1, $\Phi_f=2.10\%$ for 1b). Furthermore, the PC 1 family had a higher Φ_f when compared to the PC 2 family ($\Phi_f=0.56\%$ for 2, $\Phi_f=1.74\%$ for 2b). While an increase in nonradiative decay pathways might be predicted from the addition of flexible, freely rotating alkyl core substituents, an increase in Φ_f is instead promoted. The observed increase in Φ_f in the AkCS PCs is consistent with prior work demonstrating that CT states can minimize radiative decay. 39

Transient Absorption Spectroscopy. While the identity and duration of excited states have been found to be influential in determining PC performance in O-ATRP,26 the excitedstate lifetimes of AkCS dihydrophenazine PCs had not been evaluated prior to this work. The kinetic studies herein suggest that AkCS PCs are the dominant species after the beginning of the polymerization, and as such, the excited-state lifetimes of the AkCS PCs are expected to have a significant influence on O-ATRP outcomes. The triplet excited state is proposed to be the most catalytically relevant in our system, 26,42 consequently, the triplet excited-state lifetime (τ_{T1}) will impact polymerization control. However, the singlet excited-state lifetime (τ_{S1}) is still relevant at high substrate concentrations in dihydrophenazine PCs and is associated with a higher reaction driving force because of the higher $E^{\circ *}$ of singlet excited states relative to triplet.⁴² In comparison to the parent PCs, both AkCS PCs have a longer τ_{S1} (τ_{S1} = 8.5 ns for 1, τ_{S1} = 4.0 ns for **2**; $\tau_{S1} = 10$ ns for **1b**, $\tau_{S1} = 7.9$ for **2b**). Interestingly, PC **1** has a longer τ_{S1} than PC 2, and PC 1b has a longer τ_{S1} than PC 2b. This suggests that both the alkyl substituents and the N-aryl group influence decay pathways from the singlet state, including but not limited to ISC.

Next considering the τ_{T1} , both AkCS PCs were found to have longer lifetimes than the corresponding parent PCs, with the increase in τ_{T1} with AkCS being much more pronounced for PCs 2 and 2b (τ_{T1} = 3.3 μ s for 2, τ_{T1} = 33 μ s for 2b) than for PCs 1 and 1b ($\tau_{\rm T1}$ = 0.61 $\mu \rm s$ for 1, $\tau_{\rm T1}$ = 1.4 $\mu \rm s$ for 1b). We initially hypothesized that AkCS would shorten au_{T1} due to the freely rotating alkyl group, increasing access to nonradiative decay pathways. Based on increased τ_{T1} with AkCS, we instead propose that the addition of bulky alkyl groups to the core adds rigidity to the N-aryl group, where the triplet excited state is most likely located, due to steric constraints. Comparing the PCs with different N-aryl groups, the τ_{T1} of PC 2 was longer than that of PC 1, and the τ_{T1} of PC 2b was substantially longer than that of PC 1b, opposite of the trend observed with τ_{S1} . Notably, the lifetime of PC **2b** is comparable to the lifetimes of ArCS PCs with CT to the core substituent.³³ While currently, there is no evidence to support CT to the alkyl core substituent, this result indicates that AkCS has a significant influence on the character and duration of the excited states. Further exploration is needed to elucidate how AkCS is altering the population of excited states and leverage the effects for extended τ_{T1} and improved PC performance. Overall, the observed changes in PC excited states with AkCS support the evolution of PC properties.

Redox Properties. Both $E^{\circ*}$ and $PC^{\bullet+}$ $E_{1/2}$ are critical to maintaining polymerization control in O-ATRP. Balancing these two intrinsically related properties to promote fast activation and maintain efficient deactivation is an essential part of PC design. Based on the increase in the rate of AkCS from the first to second substitution in both PCs, we

hypothesized that $E^{\circ *}$ would increase with AkCS. Instead, the singlet excited-state reduction potentials $(E_{S1}^{\circ *})$ for the AkCS PCs $(E_{S1}^{\circ *} = -1.70 \text{ V vs SCE for } 1b, E_{S1}^{\circ *} = -1.73 \text{ V}$ vs SCE for 2b) were not significantly different from those of the parent PCs ($E_{S1}^{\circ *} = -1.70 \text{ V}$ vs SCE for 1, $E_{S1}^{\circ *} = -1.72$ V vs SCE for 2). This observation suggests that the driving force for activation is not responsible for the increase in the rate between the first and second substitution, and instead, another catalytically relevant property (ex. $PC^{\bullet+}$ $E_{1/2}$ or excited-state lifetime) may be dominant. Further supporting that $E_{S1}^{\circ *}$ does not determine the rate of substitution, the $E_{\rm S1}^{\ \ \circ *}$ for PC 2 was higher than that for PC 1, but PC 1 exhibited faster core substitution. PC **2b** had the highest $E_{S1}^{\circ *}$, which in combination with long au_{T1} and high $arepsilon_{\mathrm{max,abs}}$ indicates that this PC should be the highest performing PC in O-ATRP. Recalling that the E_{T1} was measured at 77 K, which explains why the $E_{\text{T1}}^{\circ*}$ is higher than $E_{\text{S1}}^{\circ*}$ in these PCs, relative trends in $E_{\rm T1}{}^{\circ *}$ can still be evaluated. Similar to the trend observed in $E_{\rm S1}^{\circ *}$, the $E_{\rm T1}^{\circ *}$ values of the AkCS PCs ($E_{\rm T1}^{\circ *}$ = -1.96 V vs SCE for 1b, $E_{T1}^{\circ *} = -2.04 \text{ V}$ vs SCE for 2b) were lower than the $E_{\rm T1}^{\circ *}$ of the respective parent PCs ($E_{\rm T1}^{\circ *}$ = -2.02 V vs SCE for 1, $E_{T1}^{\circ *} = -2.13 \text{ V vs SCE for 2}$), and the $E_{T1}^{\circ *}$ of PC 2 was higher than PC that of 1. Overall, the $E^{\circ *}$ values were not improved significantly by AkCS and are not likely to be the source of differences in the rates of AkCS or PC performance.

We then examined the PC $^{\bullet +}$ $E_{1/2}$, the driving force for deactivation in O-ATRP (Table 2). Comparing PCs 1 and 2,

Table 2. Summary of the Redox Properties for PCs

PC	$E_{1/2} (^{2}PC^{\bullet+}/^{1}PC)$ (V vs SCE) ^a	$E_{\text{S1}}^{\circ*}(^{2}\text{PC}^{\bullet+}/^{1}\text{PC}^{*})$ (V vs SCE) ^b	$E_{\text{T1}}^{\circ*}(^{2}\text{PC}^{\bullet+}/^{3}\text{PC}^{*})$ (V vs SCE) ^b
1	0.22	-1.70	-2.02
1b	0.27	-1.70	-1.96
2	0.21	-1.72	-2.13
2b	0.26	-1.73	-2.04

^aFirst oxidation potential measured in DMAc with NBu₄PF₆ as the electrolyte. ^bSinglet and triplet excited-state reduction potentials were determined from the $E_{1/2}$ and singlet (E_{S1}) and triplet (E_{T1}) energies, respectively (see the SI for more details).

the PC $^{\bullet+}$ $E_{1/2}$ values were comparable ($E_{1/2} = 0.22 \text{ V vs SCE}$ for 1, $E_{1/2}$ = 0.21 V vs SCE for 2). With AkCS, $E_{1/2}$ increased from the parent PCs for both PCs **1b** and **2b** ($E_{1/2} = 0.27 \text{ V vs}$ SCE for 1b, $E_{1/2} = 0.26$ V vs SCE for 2b). The increase with AkCS was surprising given the mildly electron-donating character of the alkyl groups, which is expected to stabilize PC* and make it less oxidizing. However, the two esters on DBMM may be inductively withdrawing enough to destabilize the PC $^{\bullet+}$. Just as the PC $^{\bullet+}$ $E_{1/2}$ values were very similar between PCs 1 and 2, the AkCS PC $^{\bullet+}$ $E_{1/2}$ values are also within 0.01 V, indicating that the connectivity of the Nnaphthyl group in PC 1 vs 2 does not have a strong influence on deactivation, while the core substituent has a moderate effect. A higher $PC^{\bullet+}$ $E_{1/2}$ promotes radical addition through the PC*+ after the activation step and may explain why the second substitution is faster than the first. This observation also suggests that the radical addition step in AkCS is more likely to be rate-limiting than SET. However, the small differences observed between PCs 1 and 2 suggest that PC*+ $E_{1/2}$ is not strongly influential in determining the faster rate of AkCS observed with PC 1 vs 2. The increase in PC $^{\bullet+}$ $E_{1/2}$ with

AkCS supports the hypothesis that PC properties are evolving and, in several cases, improving through AkCS.

In summary, photophysical and redox characterization of the parent and AkCS PCs showed that most PC properties were modified through AkCS with R*. Several properties that are correlated with superior performance in O-ATRP improved with AkCS, including $\varepsilon_{\rm max,abs}$, excited-state lifetimes, and PC*+ $E_{1/2}$. Observation of modified properties in PCs 1b and 2b supports the hypothesis that PC properties are evolving and demonstrates that the relevant properties for most of the polymerization are those of the core-substituted PCs. The higher PC $^{\bullet+}$ $E_{1/2}$ observed in the disubstituted PCs compared to parent PCs could explain the increase in the AkCS rate if the radical addition step of AkCS is rate-limiting rather than activation. To explore the possibility of radical addition as the rate-limiting step, second-order kinetic plots were examined for each PC substitution and were found to have reasonable fits, albeit worse than the fits for the pseudo-first-order plots in most cases (Figures S31 and S32). Overall, a definitive correlation between changes in PC properties and the increase in the substitution rate between the first and second substitution is still not fully elucidated, and further investigation is needed to determine the rate-limiting step in AkCS. The reason for the increase in the AkCS rate with 1naphthyl versus 2-naphthyl also merits an additional study. One possibility is that the longer donor-acceptor distance in PC 2 is associated with a larger reorganization energy as observed for analogous phenoxazine PCs, which could slow electron transfer or radical addition.³⁷

Application of PCs in O-ATRP. After evaluating the influence of AkCS on PC properties, we wanted to assess whether faster access to modified properties (as indicated by the rate of substitution) or the PC properties themselves are more important in determining polymerization control. We hypothesized that faster AkCS would result in better performance in O-ATRP. To explore this hypothesis, O-ATRP of methyl methacrylate (MMA) was performed with each PC in DMAc with DBMM as the initiator (Table 3).

Table 3. O-ATRP Results Using PCs 1, 2, 1b, and 2b for the Polymerization of MMA^a

PC	solvent	conv. (%) ^b	$M_{\rm n, theo}({ m kDa})^{b}$	$M_{\rm n,\ exp}({ m kDa})^c$	$\mathbf{\tilde{D}}^{c}$	I* (%) ^d
1	DMAc	87.1	8.97	10.1	1.15	89
1b	DMAc	91.3	9.39	10.2	1.12	92
2	DMAc	86.4	8.90	9.84	1.17	90
2b	DMAc	87.1	9.48	9.50	1.14	100
1	EtOAc	84.1	8.68	10.6	1.05	82
1b	EtOAc	87.5	9.01	8.79	1.07	102
2	EtOAc	79.5	8.21	8.22	1.04	100
2b	EtOAc	80.5	8.32	8.67	1.05	96

^aReaction scheme for O-ATRP of MMA catalyzed by PCs 1, 2, 1b, and 2b. Conditions: [MMA]:[DBMM]:[PC] = [1000]:[10]:[1], 1.00 mL of solvent (DMAc or EtOAc), 1.00 mL of MMA. O-ATRP was run with a white LED beaker as the light source (see the SI for more information). ^bConversion determined by ¹H NMR at 8 (DMAc) or 24 h (EtOAc). ^cDetermined by GPC with multiangle light scattering. ^dI* = $(M_{n, theo}/M_{n, exp}) \times 100$.

Comparing the performance of parent PCs 1 and 2 in DMAc, 1 and 2 have similar \mathcal{D} and I^* at 8 h ($\mathcal{D}=1.15$, $I^*=89\%$ for 1, $\mathcal{D}=1.17$, $I^*=90\%$ for 2). However, PC 1 demonstrates significantly better control at early reaction times than PC 2 based on plots of M_n versus conversion, suggesting that faster core substitution promotes access to PC 1b and consequently improved PC properties early on (Figures S77 and S79). Alternatively, the superior control of PC 1 at early times could be a result of faster PC* generation, which serves as a supplemental deactivator. 31,43

Polymerization control in O-ATRP was also evaluated with EtOAc as the solvent. Using a less polar solvent than DMAc (THF or EtOAc) has been found to improve O-ATRP outcomes in prior works. 31,34 This effect is proposed to be the result of PC++ destabilization in less polar solvents, which encourages ion pairing and increases $PC^{\bullet+}$ $E_{1/2}$, resulting in more efficient deactivation. Decreased solvent polarity also commonly improves properties related to activation by increasing Φ_{ISC} , decreasing nonradiative decay, and increasing excited-state lifetimes.³¹ As expected, O-ATRP in EtOAc resulted in a lower D for each PC compared to DMAc. However, PCs 1 and 2b had slightly lower I* values in EtOAc than in DMAc (Table 3). Comparing PCs 1 and 2 in EtOAc, PC 1 exhibits lower I^* at 24 h ($I^* = 82\%$, D = 1.05) than PC 2 $(I^* = 100\%, D = 1.04)$. However, PC 1 shows better control at early reaction times in EtOAc compared to PC 2 based on plots of M_n versus conversion (Figure 5). Together, these

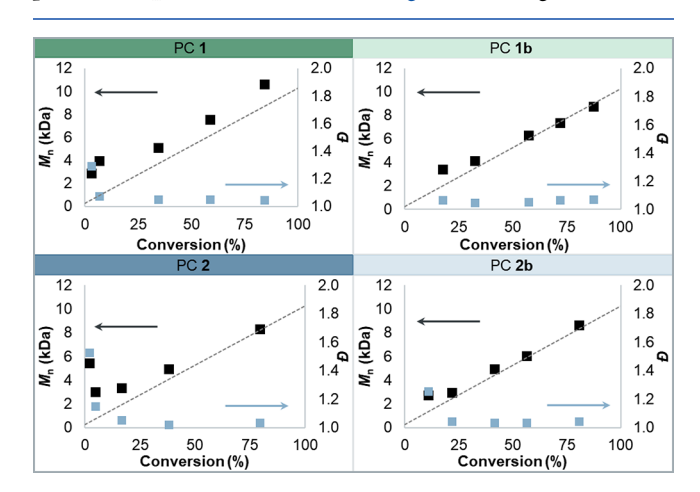


Figure 5. Plots of the growth of polymer $M_{\rm n}$ as a function of monomer (MMA) conversion to polymer (black squares) and ${\cal D}$ (blue squares, secondary *y*-axis) for each time point (2, 4, 8, 12, and 24 h) in EtOAc. $M_{\rm nv}$ theo values are represented by the gray dashed line.

observations support the hypothesis that faster AkCS results in better control but indicate that the effect is most influential at early polymerization times. At later reaction times, PCs 1 and 2 have been core-substituted to PCs 1b and 2b, and the rate of AkCS no longer dominates polymerization control. This could explain why PC 2, which evolves to PC 2b with the best PC properties, has better control at high conversions in comparison to PC 1. The consistent difference in PC performance between the PC 2 and PC 1 families suggests that the *N*-aryl group connectivity influences polymerization outcomes for both the parent and AkCS PCs.

Based on the improved $E_{1/2}$ and τ_{T1} observed in AkCS PCs, we hypothesized that AkCS would overall increase polymer-

ization control in O-ATRP. Comparing the performance of PC 1 to 1b in DMAc at 8 h, AkCS resulted in comparable D and I^* (D = 1.15, $I^* = 89\%$ for 1, D = 1.12, $I^* = 92\%$ for 1b). Between PCs 2 and 2b, I^* improved with AkCS, and D was similar (D = 1.17, $I^* = 90\%$ for $\mathbf{2}$, D = 1.14, $I^* = 100\%$ for $\mathbf{2b}$), indicating that AkCS can improve polymerization control. However, the plots of M_n vs conversion show that the AkCS PCs deviate from a linear trend at early time points in comparison to the parent PCs, indicating less control at the beginning of the polymerization (Figures S78 and S80). Loss of control at early times with PCs 1b and 2b may result from eliminating the AkCS side reaction as a source of PC*+ buildup early in the polymerization, which helps drive deactivation to improve control. 43 AkCS PCs also reached higher conversions than parent PCs, likely another effect from the suppression of the AkCS side reaction (Table 3).

For the polymerizations in EtOAc, PC 1b had a similar D to PC 1 (D = 1.05 for 1, D = 1.07 for 1b) but a higher I^* of 102% compared to 82% for PC 1 at 24 h. PC 1b also had better control at early times than PC 1 as shown by the plot of M_n vs conversion and maintained a lower D throughout the polymerization (Figure 5). PC 2 and PC 2b show nearly identical D and I^* in EtOAc at 24 h (D = 1.04, $I^* = 100\%$ for 2, D = 1.05, $I^* = 96\%$ for 2b), indicating excellent control at high conversions for both PCs. At early reaction times, PC 2b demonstrates a substantially more linear relationship between M_n and conversion than PC 2 as well as a lower \mathcal{D} (Figure 5). For both PC families, the AkCS PCs demonstrated better overall polymerization control than the parent PCs, supporting the hypothesis that AkCS improves PC performance in O-ATRP. Notably, in EtOAc, PC 1 and PC 1b perform better at early times than PC 2 and PC 2b, respectively. The observation that AkCS PCs show better control in the plots of M_n versus conversion over parent PCs in EtOAc while the opposite trend was observed in DMAc suggests that solvent polarity alters which effect dominates PC performance. We hypothesize that in the less polar solvent (EtOAc), AkCS PCs with improved PC properties exhibit overall better polymerization control because solvent effects that bolster catalytically relevant properties will dominate (ex. extended τ_{T1}). In DMAc, the effect of additional PC*+ generated through AkCS seems more influential and may explain the improved control of the parent PCs at early times, although the AkCS PCs still perform better at high conversions.

Since AkCS N,N-diaryl dihydrophenazine PCs have been shown to effectively mediate O-ATRP at low PC loadings in previous works, ^{32–34} the ability of AkCS PC **2b** to maintain polymerization control at PC loadings of <1000 ppm was evaluated (Table 4). O-ATRP down to 250 ppm PC showed minimal loss in polymerization control ($D = 1.12, I^* = 96\%$), and moderate control was maintained at 50 ppm ($\bar{D} = 1.30, I^*$ = 96%). The ability of the AkCS PC to maintain polymerization control at low PC loadings indicates that 2b is a robust, high-performing PC. Additionally, the results show that lower PC loadings may minimize the AkCS side reaction and consequently result in higher I* if overall polymerization control is maintained (ex. $I^* = 96\%$ at 1000 ppm; $I^* = 100\%$ at 500 ppm), an effect also observed in prior work.³⁴ To determine if AkCS PC 2b can achieve higher molecular weights while maintaining control, polymerizations targeting a degree of polymerization (DP) of 250, 500, and 1000 were performed. While polymerization control was maintained at a DP of 250 (D = 1.18, $I^* = 96\%$), it was lost at DP = 500 and

Table 4. O-ATRP Results Using PC 2b for Polymerization of MMA at Varied PC Loadings^a

PC loading (ppm)	conv. (%) ^b	$M_{\rm n, theo}({ m kDa})^b$	$M_{ m n, exp}({ m kDa})^c$	$\boldsymbol{\mathcal{D}^c}$	I*(%) ^d
1000	80.5	8.32	8.67	1.05	96
500	78.6	8.13	8.11	1.08	100
250	88.2	9.08	9.47	1.12	96
100	92.9	9.56	9.46	1.21	101
50	94.6	9.72	10.11	1.30	96
25	91.2	9.38	9.44	1.55	99
10	77.0	7.96	18.91	1.49	42

^aConditions: [MMA]:[DBMM] = [1000]:[10], PC loading is relative to mols of monomer, 1.00 mL of EtOAc, 1.00 mL of MMA. O-ATRP was run with a white LED beaker as the light source (see the SI for more information). ^bConversion determined by ¹H NMR at 24 h. ^cDetermined by GPC with multiangle light scattering, ^dI* = $(M_{\rm n, theo}/M_{\rm n, exp}) \times 100$.

1000, suggesting that the AkCS PCs are not suited for the controlled polymerization of high-molecular-weight polymers under these conditions (Table S1). Overall, the polymerization data show that AkCS can be leveraged to achieve improved polymerization control even at low catalyst loadings, especially in low-polarity solvents that enhance PC properties.

CONCLUSIONS

This work highlights an important consideration for O-ATRP mediated by unsubstituted dihydrophenazine PCs (ex. PCs 1 and 2), which are often utilized in O-ATRP. The parent PC and associated PC properties are only exclusively relevant at the beginning of the reaction, and as the polymerization proceeds, AkCS PCs with properties distinct from those of the parent PCs were found to rapidly form. The rate of AkCS was influenced by N-aryl group connectivity, with PC 1 undergoing faster AkCS than PC 2. Observation of faster AkCS for PC 1 improves our understanding of why PCs 1 and 2 perform differently in O-ATRP, but further investigation is needed to determine the cause of the faster substitution rate in PC 1.

Additionally, the second substitution of DBMM fragments to the PC core was found to be faster than the first, indicating the evolution of PC properties upon AkCS. The evolution of PC properties was supported by PC characterization, which revealed that AkCS alters both photophysical and redox properties. Importantly, longer τ_{T1} and higher PC $^{\bullet+}$ $E_{1/2}$ were observed ($\tau_{\text{T1}} = 1.4 - 33 \,\mu\text{s}$, $E_{1/2} = 0.26 - 0.27 \,\text{V}$ vs SCE), with the improved $E_{1/2}$ upon AkCS potentially explaining increases in the rate after the first substitution if radical addition is ratelimiting. The rate of AkCS was found to be more important in determining polymerization control at early reaction times, while at later reaction times, the properties of the PCs accessed were more influential, especially in EtOAc. AkCS PCs were found to perform better in O-ATRP based on I^* ($I^* = 92$ -102%) and plots of M_n vs conversion when compared to parent PCs ($I^* = 82-100\%$), again particularly in EtOAc, which has been found to enhance PC properties. Additionally, an AkCS PC was able to maintain polymerization control at PC loadings of as low as 50 ppm.

Broadly, this work has improved the fundamental understanding of AkCS in dihydrophenazine PCs and advanced the development of PCs for use in O-ATRP. We envision radical addition to the core as a facile pathway to tune organic PC structure and properties while simultaneously minimizing

undesirable side reactivity. Insights from this work, including an improved understanding of excited-state lifetimes and the influence of *N*-aryl connectivity, will direct future efforts in the design of organic PCs that are relevant to both O-ATRP and the wider field of photoredox catalysis.

ASSOCIATED CONTENT

Supporting Information

The Supporting Information is available free of charge at https://pubs.acs.org/doi/10.1021/acscatal.3c04060.

Materials and methods, supplemental polymerization data, PC characterization, and procedures for syntheses, kinetic studies, polymerizations, and PC characterization (PDF)

AUTHOR INFORMATION

Corresponding Author

Garret M. Miyake — Department of Chemistry, Colorado State University, Fort Collins, Colorado 80523, United States; orcid.org/0000-0003-2451-7090;

Email: Garret.Miyake@colostate.edu

Authors

Katherine O. Puffer – Department of Chemistry, Colorado State University, Fort Collins, Colorado 80523, United States Daniel A. Corbin – Department of Chemistry, Colorado State University, Fort Collins, Colorado 80523, United States

Complete contact information is available at: https://pubs.acs.org/10.1021/acscatal.3c04060

Notes

The authors declare no competing financial interest.

ACKNOWLEDGMENTS

This work was supported by Colorado State University, the NSF (2055742), and the NIH (R35GM119702). The content is solely the responsibility of the authors and does not necessarily represent the official views of the National Institutes of Health. The authors would like to thank Anna Wolff, Cameron Chrisman, and Mariel Price for their assistance and helpful discussions during this work and the Analytical Resources Core (RRID: SCR_021758) at Colorado State University for instrument access and training.

REFERENCES

- (1) Narayanam, J. M. R.; Stephenson, C. R. J. Visible light photoredox catalysis: applications in organic synthesis. *Chem. Soc. Rev.* **2011**, *40*, 102–113.
- (2) Prier, C. K.; Rankic, D. A.; MacMillan, D. W. C. Visible light photoredox catalysis with transition metal complexes: applications in organic synthesis. *Chem. Rev.* **2013**, *113*, 5322–5363.
- (3) Romero, N. A.; Nicewicz, D. A. Organic photoredox catalysis. *Chem. Rev.* **2016**, *116*, 10075–10166.
- (4) Corrigan, N.; Shanmugam, S.; Xu, J. T.; Boyer, C. Photocatalysis in organic and polymer synthesis. *Chem. Soc. Rev.* **2016**, *45*, 6165–6212.
- (5) Yoon, T. P.; Ischay, M. A.; Du, J. N. Visible light photocatalysis as a greener approach to photochemical synthesis. *Nat. Chem.* **2010**, 2, 527–532.
- (6) Arias-Rotondo, D. M.; McCusker, J. K. The photophysics of photoredox catalysis: a roadmap for catalyst design. *Chem. Soc. Rev.* **2016**, *45*, 5803–5820.
- (7) Koyama, D.; Dale, H. J. A.; Orr-Ewing, A. J. Ultrafast observation of a photoredox reaction mechanism: photoinitiation in organo-

- catalyzed atom-transfer radical polymerization. J. Am. Chem. Soc. 2018, 140, 1285–1293.
- (8) Corbin, D. A.; Swisher, N. A.; Miyake, G. M. Fundamentals of Photochemical Redox Reactions. In *Organic Redox Chemistry: Chemical, Photochemical, and Electrochemical Syntheses,* 1st ed; Wiley-VCH, 2021; pp 45–102.
- (9) Theriot, J. C.; McCarthy, B. G.; Lim, C. H.; Miyake, G. M. Organocatalyzed atom transfer radical polymerization: perspectives on catalyst design and performance. *Macromol. Rapid Commun.* **2017**, 38, 1700040.
- (10) Ludwig, J. R.; Schindler, C. S. Catalyst: sustainable catalysis. *Chem.* **2017**, *2*, 313–316.
- (11) Corbin, D. A.; Lim, C. H.; Miyake, G. M. Phenothiazines, dihydrophenazines, and phenoxazines: sustainable alternatives to precious-metal-based photoredox catalysts. *Aldrichim. Acta* **2019**, *52*, 7–21.
- (12) Theriot, J. C.; Lim, C. H.; Yang, H.; Ryan, M. D.; Musgrave, C. B.; Miyake, G. M. Organocatalyzed atom transfer radical polymerization driven by visible light. *Science* **2016**, *352*, 1082–1086.
- (13) Pearson, R. M.; Lim, C. H.; McCarthy, B. G.; Musgrave, C. B.; Miyake, G. M. Organocatalyzed atom transfer radical polymerization using *N*-aryl phenoxazines as photoredox catalysts. *J. Am. Chem. Soc.* **2016**, 138, 11399–11407.
- (14) Valle, M.; Ximenis, M.; de Pariza, X. L.; Chan, J. M. W.; Sardon, H. Spotting trends in organocatalyzed and other organomediated (de)polymerizations and polymer functionalizations. *Angew. Chem., Int. Ed.* **2022**, *61*, No. e202203043.
- (15) Wu, C.; Corrigan, N.; Lim, C. H.; Liu, W.; Miyake, G.; Boyer, C. Ration design of photocatalysts for controlled polymerization: effect of structures of photocatalytic activites. *Chem. Rev.* **2022**, *122*, 5476–5518.
- (16) Wang, J. S.; Matyjaszewski, K. Controlled living radical polymerization atom-transfer radical polymerization in the presence of transition-metal complexes. *J. Am. Chem. Soc.* **1995**, *117*, 5614–5615.
- (17) Kato, M.; Kamigaito, M.; Sawamoto, M.; Higashimura, T. Polymerization of methyl-methacrylate with the carbon-tetrachloride dichlorotris(triphenylphosphine)ruthenium(II) methylaluminum bis-(2,6-di-tert-butylphenoxide) initiating system possibility of living radical polymerization. *Macromolecules* 1995, 28, 1721–1723.
- (18) Discekici, E. H.; Anastasaki, A.; de Alaniz, J. R.; Hawker, C. J. Evolution and future directions of metal-free atom transfer radical polymerization. *Macromolecules* **2018**, *51*, 7421–7434.
- (19) Corbin, D. A.; Miyake, G. M. Photoinduced organocatalyzed atom transfer radical polymerization (O-ATRP): precision polymer synthesis using organic photoredox catalysis. *Chem. Rev.* **2022**, *122*, 1830–1874.
- (20) Ramakers, G.; Krivcov, A.; Trouillet, V.; Welle, A.; Mobius, H.; Junkers, T. Organocatalyzed photo-atom transfer radical polymerization of methacrylic acid in continuous flow and surface grafting. *Macromol. Rapid Commun.* **2017**, *38*, 1700423.
- (21) Treat, N. J.; Sprafke, H.; Kramer, J. W.; Clark, P. G.; Barton, B. E.; de Alaniz, J. R.; Fors, B. P.; Hawker, C. J. Metal-free atom transfer radical polymerization. *J. Am. Chem. Soc.* **2014**, *136*, 16096–16101.
- (22) Matyjaszewski, K.; Tsarevsky, N. V. Macromolecular engineering by atom transfer radical polymerization. *J. Am. Chem. Soc.* **2014**, 136, 6513–6533.
- (23) Matyjaszewski, K. Atom transfer radical polymerization (ATRP): current status and future perspectives. *Macromolecules* **2012**, *45*, 4015–4039.
- (24) Chen, M.; Zhong, M. J.; Johnson, J. A. Light-controlled radical polymerization: mechanisms, methods, and applications. *Chem. Rev.* **2016**, *116*, 10167–10211.
- (25) Poelma, S. O.; Burnett, G. L.; Discekici, E. H.; Mattson, K. M.; Treat, N. J.; Luo, Y. D.; Hudson, Z. M.; Shankel, S. L.; Clark, P. G.; Kramer, J. W.; Hawker, C. J.; de Alaniz, J. R. chemoselective radical dehalogenation and C-C bond formation on aryl halide substrates using organic photoredox catalysts. *J. Org. Chem.* **2016**, *81*, 7155–7160.

- (26) Du, Y.; Pearson, R. M.; Lim, C. H.; Sartor, S. M.; Ryan, M. D.; Yang, H. S.; Damrauer, N. H.; Miyake, G. M. Strongly reducing, visible-light organic photoredox catalysts as sustainable alternatives to precious metals. *Chem. Eur. J.* **2017**, *23*, 10962–10968.
- (27) McCarthy, B. G.; Pearson, R. M.; Lim, C. H.; Sartor, S. M.; Damrauer, N. H.; Miyake, G. M. Structure-property relationships for tailoring phenoxazines as reducing photoredox catalysts. *J. Am. Chem. Soc.* **2018**, *140*, 5088–5101.
- (28) Miyake, G. M.; Theriot, J. C. Perylene as an organic photocatalyst for the radical polymerization of functionalized vinyl monomers through oxidative quenching with alkyl bromides and visible light. *Macromolecules* **2014**, *47*, 8255–8261.
- (29) Buss, B. L.; Lim, C. H.; Miyake, G. M. Dimethyl dihydroacridines as photocatalysts in organocatalyzed atom transfer radical polymerization of acrylate monomers. *Angew. Chem., Int. Ed.* **2020**, *59*, 3209–3217.
- (30) Corbin, D. A.; Cremer, C.; Puffer, K. O.; Newell, B. S.; Patureau, F. W.; Miyake, G. M. Effects of the chalcogenide identity in *N*-aryl phenochalcogenazine photoredox catalysts. *ChemCatChem.* **2022**, *14*, No. e202200485.
- (31) McCarthy, B.; Sartor, S.; Cole, J.; Damrauer, N.; Miyake, G. M. Solvent effects and side reactions in organocatalyzed atom transfer radical polymerization for enabling the controlled polymerization of acrylates catalyzed by diaryl dihydrophenazines. *Macromolecules* **2020**, 53, 9208–9219.
- (32) Cole, J. P.; Federico, C. R.; Lim, C. H.; Miyake, G. M. Photoinduced organocatalyzed atom transfer radical polymerization using low ppm catalyst loading. *Macromolecules* **2019**, *52*, 747–754.
- (33) Price, M. J.; Puffer, K. O.; Kudisch, M.; Knies, D.; Miyake, G. M. Structure-property relationships of core-substituted diaryl dihydrophenazine organic photoredox catalysts and their application in O-ATRP. *Polym. Chem.* **2021**, *12*, 6110–6122.
- (34) Corbin, D. A.; Puffer, K. O.; Chism, K. A.; Cole, J. P.; Theriot, J. C.; McCarthy, B. G.; Buss, B. L.; Lim, C. H.; Lincoln, S. R.; Newell, B. S.; Miyake, G. M. Radical addition to *N,N*-diaryl dihydrophenazine photoredox catalysts and implications in photoinduced organocatalyzed atom transfer radical polymerization. *Macromolecules* **2021**, 54, 4507–4516.
- (35) Zhang, Y. J.; Jiang, D. D.; Fang, Z.; Zhu, N.; Sun, N. X.; He, W.; Liu, C. K.; Zhao, L. L.; Guo, K. Photomediated core modification of organic photoredox catalysts in radical addition: mechanism and applications. *Chem. Sci.* **2021**, *12*, 9432–9441.
- (36) Ryan, M. D.; Theriot, J. C.; Lim, C. H.; Yang, H. S.; Lockwood, A. G.; Garrison, N. G.; Lincoln, S. R.; Musgrave, C. B.; Miyake, G. M. Solvent effects on the intramolecular charge transfer character of *N*,*N*-diaryl dihydrophenazine catalysts for organocatalyzed atom transfer radical polymerization. *J. Polym. Sci., Polym. Chem.* **2017**, *55*, 3017–3027.
- (37) Sartor, S. M.; Lattke, Y. M.; McCarthy, B. G.; Miyake, G. M.; Damrauer, N. H. Effects of naphthyl connectivity on the photophysics of compact organic charge-transfer photoredox catalysts. *J. Phys. Chem. A* **2019**, *123*, 4727–4736.
- (38) Lim, C. H.; Ryan, M. D.; McCarthy, B. G.; Theriot, J. C.; Sartor, S. M.; Damrauer, N. H.; Musgrave, C. B.; Miyake, G. M. Intramolecular charge transfer and ion pairing in *N,N*-diaryl dihydrophenazine photoredox catalysts for efficient organocatalyzed atom transfer radical polymerization. *J. Am. Chem. Soc.* **2017**, *139*, 348–355.
- (39) Sartor, S. M.; McCarthy, B. G.; Pearson, R. M.; Miyake, G. M.; Damrauer, N. H. Exploiting charge-transfer states for maximizing intersystem crossing yields in organic photoredox catalysts. *J. Am. Chem. Soc.* **2018**, 140, 4778–4781.
- (40) Lee, J.; Shizu, K.; Tanaka, H.; Nakanotani, H.; Yasuda, T.; Kaji, H.; Adachi, C. Controlled emission colors and singlet-triplet energy gaps of dihydrophenazine-based thermally activated delayed fluorescence emitters. *J. Mater. Chem. C* **2015**, *3*, 2175–2181.
- (41) Lewis, G. N.; Calvin, M. The color of organic substances. *Chem. Rev.* **1939**, *25*, 273–328.

- (42) Lattke, Y. M.; Corbin, D. A.; Sartor, S. M.; McCarthy, B. G.; Miyake, G. M.; Damrauer, N. H. Interrogation of O-ATRP activation conducted by singlet and triplet excited states of phenoxazine photocatalysts. *J. Phys. Chem. A* **2021**, *125*, 3109–3121.
- (43) Corbin, D. A.; McCarthy, B. G.; van de Lindt, Z.; Miyake, G. M. Radical cations of phenoxazine and dihydrophenazine photoredox catalysts and their role as deactivators in organocatalyzed atom transfer radical polymerization. *Macromolecules* **2021**, *54*, 4726–4738.